Scattering of microwave photons in superconducting transmission-line resonators coupled to charge qubits

Guang-Yin Chen,[1] Meng-Han Liu,[2] and Yueh-Nan Chen[2,*]

[1]*Department of Physics, National Chung Hsing University, Taichung 402, Taiwan*
[2]*Department of Physics and National Center for Theoretical Sciences, National Cheng-Kung University, Tainan 701, Taiwan*

We investigate coherent single-microwave-photon transport in the coupled superconducting transmission lines coupled to superconducting quantum interference device based charge qubits. The Fano resonance can be observed in the scattering spectra in both the linear and nonlinear regimes of the dispersion relation of the microwave photon. We further find that the degree of the two-qubit entanglement can vary from unity to zero when the Fano resonance occurs. There exists a correspondence between the entanglement and the Fano resonance.

I. INTRODUCTION

Superconducting circuits [1,2] based on Josephson junctions can behave like two-level systems. Progress in this field has made it possible to achieve coherent interaction between the two-level system and the microwave photon by coupling the superconducting qubit to a transmission-line resonator [3–7]. The phenomena of cavity QED in superconducting circuits have also been demonstrated [3,8–10] and can be further used to couple two distant qubits [2,11]. For the superconducting quantum interference device (SQUID) based charge qubits coupled to a transmission line, measurements of the populations of individual superconducting qubits have been performed [12]. Recently, the progress in generating and measuring single microwave photons [13–19] propagating in the transmission line [20–23] has made it feasible to detect the single-photon Dicke states. Therefore, one can use this advantage to measure the qubit state through the detection of the microwave photons.

When a propagating field is coupled to an emitter, the interaction leads to the scattering of the field or the excitation of the emitter. Because of the superposition principle of quantum mechanics, the interference may occur when different exciting paths are included and leads to the variations of the profile in the scattering spectra. Fano resonance [24,25], first observed in atomic absorption, indicates that when an excited discrete state is coupled to a continuum of energy states, the scattering profile shows asymmetric line shapes due to the quantum interference. Fano resonance has been reported not only in the atomic or molecular system but also in systems containing competitive pathways such as nanostructures [26–28], metamaterials [29], refractive cores within waveguides [30,31], photonic crystals [32–34], microrings [35], and quantum dots [36].

Inspired by these advances, we study in this work the scattering spectra of a system comprising the coupled transmission line resonators coupled to two or three superconducting charge qubits. We find that the Fano resonance can occur in both the linear and nonlinear regimes of the dispersion relation of the photons. We further show that the Fano resonance stemming from the interference between the discrete and continuum states has a correspondence to two-qubit entanglement.

II. THE MODEL

Let us consider the evanescently coupled superconducting transmission-line resonators coupled to two dc-SQUID-based charge qubits [37,38], as depicted in Fig. 1. With the proper gate voltage V_g, the Cooper pair box formed by the dc SQUID with the two Josephson junctions can behave like a two-level system (charge qubit). The incident microwave-photon propagating in the transmission line would be either scattered or absorbed by the qubits.

By assuming all the transmission resonators have the same frequency ω, the Hamiltonian of the evanescently coupled transmission-line resonators can be written as

$$H_t = \hbar\omega \sum_i a_i^\dagger a_i - \hbar J \sum_i (a_i^\dagger a_{i+1} + \text{H.c.}), \quad (1)$$

where $a_i^\dagger$ (a_i) is the creation (annihilation) operator of the microwave-photon propagating in the ith resonator and J is the coupling constant representing the microwave-photon hopping from one resonator to another.

This Hamiltonian [Eq. (1)] describes a tight-binding boson model with the dispersion relation

$$\Omega_k = \omega - 2J\cos(\zeta k), \quad (2)$$

where k denotes the wave vector of the microwave photon in the resonator and ζ is the lattice constant and is set to be unity throughout this paper.

The interaction between the microwave photon propagating in the transmission resonators and the two charge qubits leads to the scattering of the photon. The total Hamiltonian of the combined charge-qubit photon system can be described as

$$H_T = \sum_{j=1,2} \hbar\Omega_j \sigma_{e_j,e_j} + \int dk \hbar\Omega_k a_k^\dagger a_k + \hbar\big(g_1 a_k \sigma_{e_1,g_1} + g_2 a_k e^{ikd}\sigma_{e_2,g_2} + \text{H.c.}\big), \quad (3)$$

where Ω_j is the energy spacing of the jth charge qubit, σ_{e_j,e_j} (σ_{e_j,g_j}) $= |e_j\rangle\langle e_j|$ ($|e_j\rangle\langle g_j|$) is the diagonal (off-diagonal) element of the qubit operator with $|e_j\rangle$ ($|g_j\rangle$), meaning the jth qubit in its excited (ground) state, and $a_k^\dagger$ is the creation operator of the k-mode propagating microwave photon. Here,

*yuehnan@mail.ncku.edu.tw
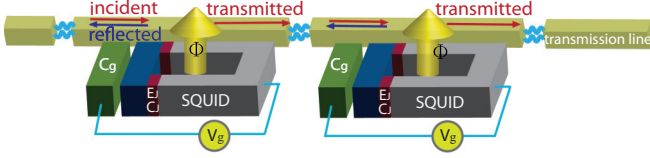
FIG. 1. (Color online) Schematic diagram of two SQUID-based charge qubits coupled to the evanescently coupled superconducting transmission-line resonators. Here C_g denotes the capacitance of the gate. The two identical Josephson junctions have capacitance C_J and coupling energy E_J. The charge qubit acts as the scattering target for the incident microwave photon, and its transition energy can be controlled by both the magnetic flux Φ threading the SQUID loop and the gate voltage V_g. Note that, depending on the interqubit distance, the charge qubits can be coupled to the same or different transmission resonators.

g_j describes the coupling strength between the field and the jth qubit, and d denotes the interqubit distance.

The stationary state of the system can be written as [39,40]

$$|E_k\rangle = \int dz [\phi_{k,R}^\dagger(z) C_R^\dagger(z) + \phi_{k,L}^\dagger(z) C_L^\dagger(z)]|\text{vac}\rangle$$
$$+ \sum_{j=1,2} \xi_{k_j} \sigma_{e_j,g_j}|\text{vac}\rangle, \qquad (4)$$

where $|\text{vac}\rangle = |g_1,g_2\rangle|0\rangle$ indicates that both the charge qubits are in the ground state with zero photons and ξ_{k_j} is the probability amplitude that the jth charge qubit absorbs the microwave photon and jumps to its excited state. We also assume that the field is incident from the left, $\phi_{k,R}^\dagger(z) \equiv e^{ikz}[\theta(-z) + \alpha\theta(z)\theta(d-z) + t\theta(z-d)]$ and $\phi_{k,L}^\dagger(z) \equiv e^{-ikz}[r\theta(-z) + \beta\theta(z)\theta(d-z)]$. Here, t and r represent the transmission and reflection amplitudes, respectively. Also, α and β are the probability amplitudes of the field between the two charge qubits (positions $z=0$ and d, respectively), and $\theta(z)$ is the unit step function.

III. FANO RESONANCE IN DIFFERENT REGIMES

At the matching condition ($\lambda \sim 4\zeta$), the dispersion relation [Eq. (2)] is approximated to be linear: $\Omega_k \simeq \omega_J \pm 2Jk$, with $\omega_J = \omega - 2J$ (in what follows, we only consider the case with positive group velocity, i.e., $\Omega_k \simeq \omega_J + 2Jk$). However, in the low-energy regime (long wavelength, $\lambda \gg \zeta$), the dispersion relation can be approximated to be parabolic: $\Omega_k = \omega_J + Jk^2$. In order to study the scattering of the incident microwave photon, the Hamiltonian H_T can be further transformed into the real-space representation $\tilde{H}$ and applied to the stationary state [41] [Eq. (4)]. The transmission spectrum $T = |t|^2$ and ξ_{k_j} in both regimes can be obtained by solving the eigenvalue equation $\tilde{H}|E_k\rangle = E_k|E_k\rangle$. The general form of the transmission spectrum in both regimes is

$$T = \frac{\Delta_1^2 \Delta_2^2}{\left(g_2^2 \Delta_1 + g_1^2 \Delta_2\right)^2 + \Delta_1^2 \Delta_2^2}. \qquad (5)$$

In the linear regime, $\Delta_j = v_g(kv_g - \Omega_j)$, with v_g being the group velocity of the microwave photon, and we have
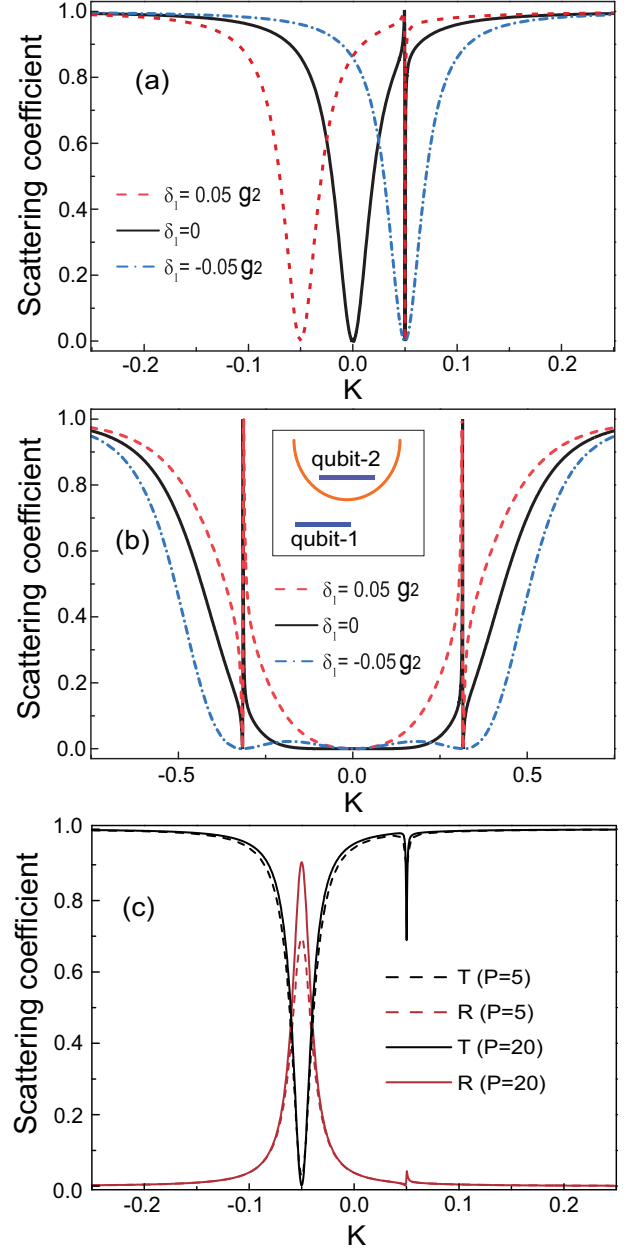
FIG. 2. (Color online) Transmission spectra of the incident microwave photon for the detuning $\delta_1 = 0.05$ (red dashed curve), 0 (black solid curve), and -0.05 (blue dot-dashed curve) in the (a) linear and (b) parabolic regimes of the dispersion relation. Here, the interqubit distance d is assumed to be much smaller than the wavelength of the incident microwave photon. (c) The transmission (black curve) and reflection (red curve) coefficients [under the same consideration as that of the red dashed curve in (a)] include dissipations for the factor $P = 5$ (dashed curve) and 20 (solid curve). The inset in (b) describes the energy configuration leading to the interference between the discrete and continuous states. The detuning δ_2 is fixed to be -0.05. Here, the ratio of the coupling strength is assumed to be $g_1/g_2 = 10$, and J is set to be 0.5. Parameters are normalized by g_2, and the normalized wave vector is defined as $K \equiv v_g k/g_2$.

defined the detuning $\delta_j \equiv \omega_J - \Omega_j$. In the parabolic regime, $\Delta_j = 2Jk(Jk^2 + \delta_j)$ with the detuning $\delta_j \equiv \omega_c - \Omega_j$ (ω_c is the minimum of the parabolic dispersion curve).

Figure 2 shows the transmission spectra T for different detuning δ_1 in both the linear and parabolic regimes of the dispersion relation. Here we have set $\delta_2 = -0.05 g_2$. The parabolic dispersion relation is similar to that in the photonic crystals [42] when ω_J is between the energies of the two qubits [$\delta_1 > 0$, $\delta_2 < 0$, as depicted in the insets of Fig. 2(b)]. Therefore, this can be viewed as the interference between the discrete and the continuous pathways and results in the Fano line shapes (red dashed and black solid curves) around the double-peak profile [41]. When $\delta_1 < 0$, the energies of the two qubits are larger than ω_c; the interference (Fano line shape) would therefore vanish (blue dot-dashed curve). Similarly, as shown in Fig. 2(a), although lacking the "band-edge-like" structure in the linear dispersion relation, when ω_J is set between Ω_1 and Ω_2, the single-peak profile in the transmission spectra also reveals the Fano line shape. This is because the two qubits play the role of the discrete states, which lead to the interference between two different pathways (red dashed and black solid curves). Similarly, as can be seen in Fig. 2(a), the Fano line shape disappears when the interference vanishes (blue dot-dashed curve). In addition, from Eq. (5), one knows that the transmission spectrum is governed by the coupling g_j and the detuning δ_j, meaning that the Fano resonance can be controlled by varying these two parameters.

Experimentally, the charge-qubit photon system is also coupled to the environment. This coupling leads to dissipations [3] such as the excited-state relaxation of the charge qubit and photon loss. To include the dissipations, we can use the "quantum jump" of an open system to modify the total Hamiltonian [39] to

$$H_T = \sum_{j=1,2} \hbar(\Omega_j - i\Gamma'/2)\sigma_{e_j,e_j} + \int dk \hbar\Omega_k a_k^\dagger a_k$$
$$+ \hbar\left(g_1 a_k \sigma_{e_1,g_1} + g_2 a_k e^{ikd}\sigma_{e_2,g_2} + \text{H.c.}\right), \quad (6)$$

where the non-Hermitian term $-i\Gamma'/2$ describes the decay from the excited state of the qubit into other dissipative channels at rate Γ'. In order to study the effect of the dissipations on scattering properties, we define a factor $P = \frac{g_1}{\Gamma'}$ and replot the red dashed curve in Fig. 2(a) for different P. As shown in Fig. 2(c), the dissipations result in lower probability of both transmission and reflection coefficients, but the their behavior remains similar. We therefore assume the dissipations are negligible in the following discussions.

IV. THE CORRESPONDENCE BETWEEN THE ENTANGLEMENT AND FANO RESONANCE

Apparently, the Fano resonance depends crucially on the energy differences between the incident microwave photon and the two charge qubits. It is interesting to investigate how the two-qubit entanglement varies when the Fano resonance occurs.

If the incident microwave-photon is not scattered but trapped between the two charge qubits, the entangled state of the two qubits can be created: $\xi_{k_1}|e_1,g_2\rangle|0\rangle + \xi_{k_2}|g_1,e_2\rangle|0\rangle$. To demonstrate the degree of the entanglement, Fig. 3 shows the concurrence [43] C of the two qubits for different detuning δ_1 (with fixed $\delta_2 = -0.05 g_2$). The concurrence quantifies the degree of the entanglement of the two qubits. For our system,
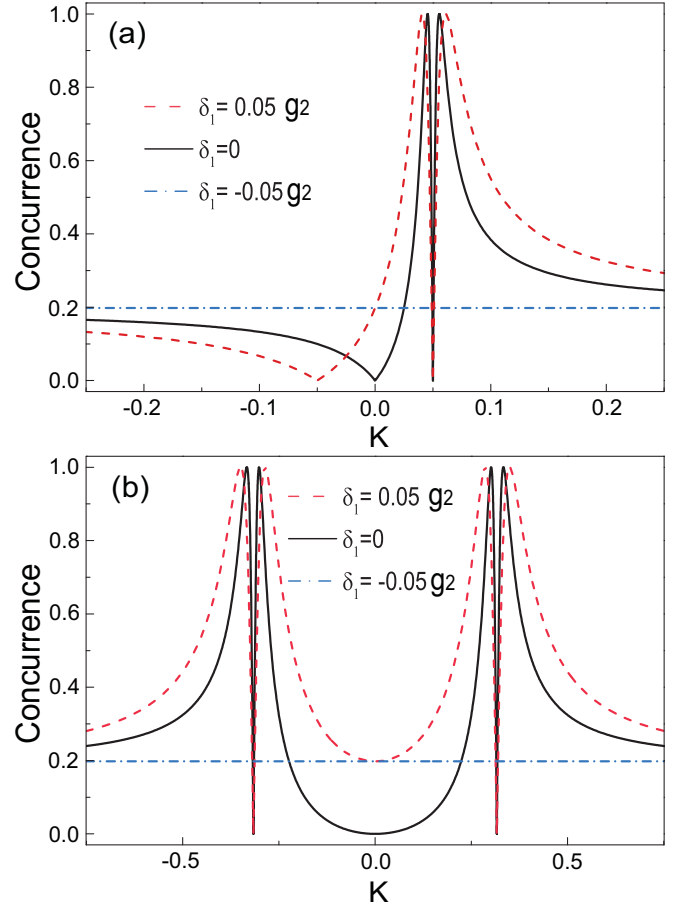
FIG. 3. (Color online) Concurrence between the two charge qubits for the detuning $\delta_1 = 0.05$ (red dashed curve), 0 (black solid curve), and -0.05 (blue dot-dashed curve) in the (a) linear and (b) parabolic regimes of the dispersion relation. Here, the interqubit distance d is assumed to be much smaller than the wavelength of the incident microwave photon. The detuning δ_2 is fixed to be -0.05. We also assume the ratio of the coupling strength $g_1/g_2 = 10$, and J is set to be 0.5. Parameters are normalized by g_2, and the normalized wave vector is defined as $K \equiv v_g k/g_2$.

after tracing out the microwave-photon modes, the reduced density matrix of the two-qubit state is a pure state, and the concurrence simply takes the form

$$C = \frac{2|\xi_{k_1}||\xi_{k_2}|}{|\xi_{k_1}|^2 + |\xi_{k_2}|^2} = \frac{2|g_2\Delta_1||g_1\Delta_2|}{g_2^2\Delta_1^2 + g_1^2\Delta_2^2}. \quad (7)$$

As can be seen in Fig. 3, the concurrence varies from unity to zero when the Fano resonance occurs in both the linear and parabolic regimes of the dispersion relation. The zero points of the Fano resonance (zero points of the transmission coefficient T) coincide with the dips of the concurrence. This can be understood from the exact solution k ($k = k_0$) for the zero points of the Fano resonance (and the concurrence): $k_0^L = \sqrt{\frac{-\delta_2}{J}}$ for the linear regime (when ω is between Ω_1 and Ω_2), and $k_0^P = \sqrt{\frac{\delta_2}{v_g}}$ for the parabolic regime.

In both regimes, the zero points of the Fano resonance occur when $\delta_2 = 0$. This point corresponds to the total reflection ($T = 0$). In this case, the second qubit takes all the excitation
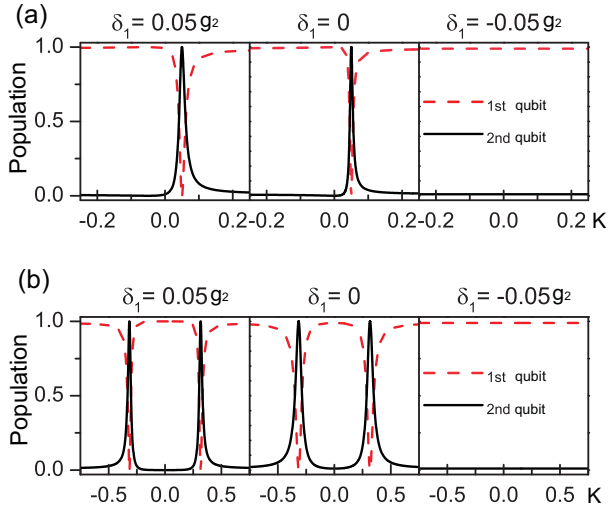
FIG. 4. (Color online) Populations of qubit 1 (red dashed curve) and qubit 2 (black solid curve) for the detuning $\delta_1 = 0.05$, 0, and -0.05 in the (a) linear and (b) parabolic regimes of the dispersion relation. Here, the interqubit distance d is assumed to be much smaller than the wavelength of the incident microwave photon. The detuning δ_2 is fixed to be -0.05. The ratio of the coupling strength is assumed to be $g_1/g_2 = 10$, and J is set to be 0.5. Parameters are normalized by g_2, and the normalized wave vector is defined as $K \equiv v_g k/g_2$.

in the two-qubit Hilbert space, as shown in Fig. 4. However, when δ_2 has nonzero negative values, the interference between the discrete and continuous channels creates the two-dip (Fano-like) line shape for the parabolic (linear) regime in the concurrence.

To get more insight on the correlations, we further study the exact solutions when the transmission and the concurrence equal to unity. The exact solutions in the linear regime for $T = 1$ read

$$k^L = \frac{g_1^2 \delta_2 + g_2^2 \delta_1}{v_g (g_1^2 + g_2^2)}, \qquad (8)$$

and the solutions for $C = 1$ can be expressed as

$$k^L = \frac{g_1 \delta_2 + g_2 \delta_1}{v_g (g_1 + g_2)} \quad \text{or} \quad k^L = \frac{g_1 \delta_2 - g_2 \delta_1}{v_g (g_1 - g_2)}, \qquad (9)$$

while the exact solutions in the parabolic regime for $T = 1$ read

$$k^P = \sqrt{\frac{-(g_1^2 \delta_2 + g_2^2 \delta_1)}{J(g_1^2 + g_2^2)}}, \qquad (10)$$

and the solutions for $C = 1$ can be expressed as

$$k^P = \sqrt{\frac{-(g_1 \delta_2 + g_2 \delta_1)}{J(g_1 + g_2)}} \quad \text{or} \quad k^P = \sqrt{\frac{-(g_1 \delta_2 - g_2 \delta_1)}{J(g_1 - g_2)}}. \qquad (11)$$

One can find that Eqs. (8) and (10) resemble Eqs. (9) and (11), respectively. This indicates that correlations exist between the two-qubit entanglement and the Fano resonance. The underlying physics is that when the Fano resonance occurs, the transmission spectrum goes down to zero and results in

the minimum of the concurrence. It then dramatically changes from zero to unity. Correspondingly, the population of qubit 1 (qubit 2) first goes down (up) and then goes up (down), and the maximum entanglement occurs when the populations of the two dots are equal, as shown in Fig. 3.

V. FANO RESONANCE AND THE CONCURRENCE WITH AN ADDITIONAL CHARGE QUBIT

In practice, it is feasible to couple more qubits to the transmission-line resonators [2]. Therefore, the Fano resonance and the bipartite entanglement would be changed in the presence of the additional qubits. Here, we consider an additional charge qubit placed next to the two qubits with the coupling strength g_3, as depicted in Fig. 5(a). Compared with
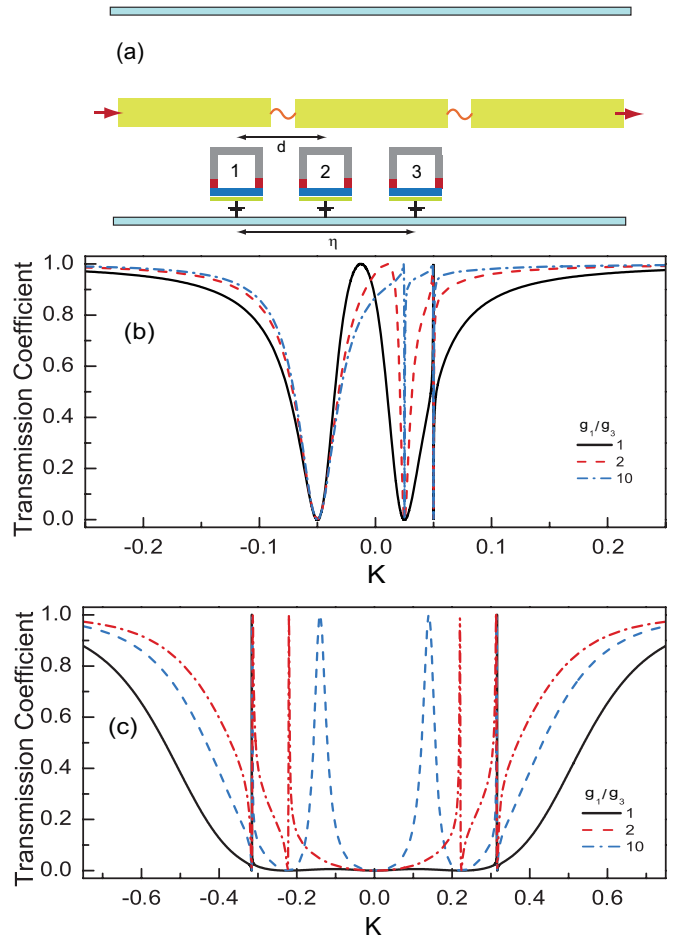
FIG. 5. (Color online) (a) Schematic diagram for the three charge qubits coupled to the coupled transmission resonators. Transmission spectra of the incident microwave photon for the ratio of the couplings $g_1/g_3 = 1$ (black solid curve), 2 (red dashed curve), and 10 (blue dot-dashed curve) in the (b) linear and (c) parabolic regimes of the dispersion relation. Here, the interqubit distances d and η are both assumed to be much smaller than the wavelength of the incident microwave photon, such that the three qubits may be coupled to the same resonator. The detuning $\delta_{1(2)}$ is fixed to be -0.05 ($+0.05$), and the detuning δ_3 is fixed to be -0.025. The ratio of the coupling strength is assumed to be $g_1/g_2 = 10$, and J is set to be 0.5. Parameters are normalized by g_2, and the normalized wave vector is defined as $K \equiv v_g k/g_2$.
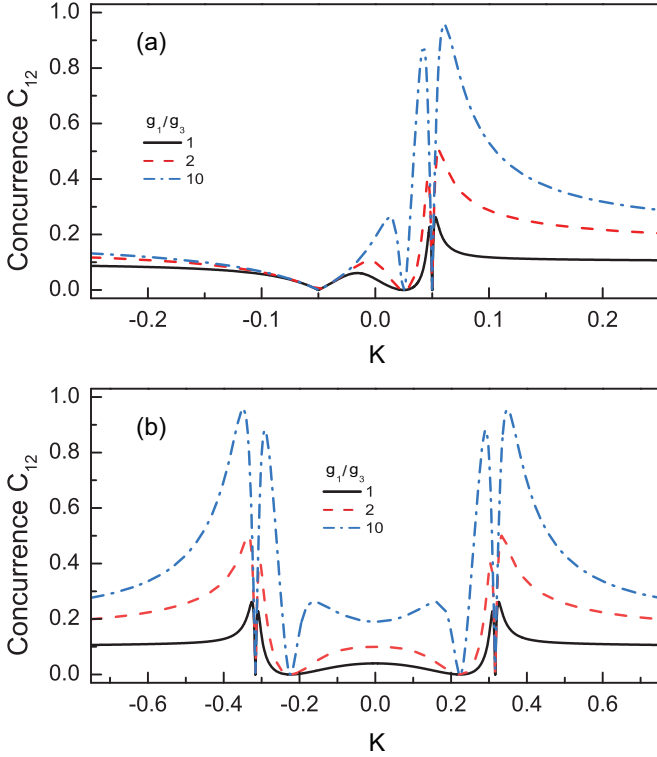
FIG. 6. (Color online) Concurrence between the first two charge qubits for the ratio of the couplings $g_1/g_3 = 1$ (black solid curve), 2 (red dashed curve), and 10 (blue dot-dashed curve) in the (a) linear and (b) parabolic regimes of the dispersion relation. Here, the interqubit distances d and η are both assumed to be much smaller than the wavelength of the incident microwave photon. The detuning $\delta_{1(2)}$ is fixed to be -0.05 ($+0.05$), and the detuning δ_3 is fixed to be -0.025. The ratio of the coupling strength is assumed to be $g_1/g_2 = 10$, and J is set to be 0.5. Parameters are normalized by g_2, and the normalized wave vector is defined as $K \equiv v_g k/g_2$.

Eq. (6), the modified Hamiltonian becomes

$$H_T = \sum_{j=1}^{3} \hbar\Omega_j \sigma_{e_j,e_j} + \int dk \hbar\Omega_k a_k^\dagger a_k + (g_1 a_k \sigma_{e_1,g_1}$$

$$+ g_2 a_k e^{ikd}\sigma_{e_2,g_2} + g_3 a_k e^{ik\eta}\sigma_{e_3,g_3} + \text{H.c.}). \quad (12)$$

The stationary state with the third qubit can be written as

$$|E_k\rangle = \int dz[\phi_{k,R}^\dagger(z)C_R^\dagger(z) + \phi_{k,L}^\dagger(z)C_L^\dagger(z)]|\text{vac}\rangle$$

$$+ \sum_{j=1}^{3} \xi_{k_j}\sigma_{e_j,g_j}|\text{vac}\rangle. \quad (13)$$

After carrying out the eigenvalue equation $\tilde{H}|E_k\rangle = E_k|E_k\rangle$ [here, $\tilde{H}$ is the real-space representation of Eq. (11)], the general three-qubit transmission coefficient in both regimes can be obtained:

$$T = \frac{(\Delta_1\Delta_2\Delta_3)^2}{(g_3^2\Delta_1\Delta_2 + g_2^2\Delta_1\Delta_3 + g_1^2\Delta_2\Delta_3)^2 + (\Delta_1\Delta_2\Delta_3)^2}. \quad (14)$$

The concurrence of the first two qubits (qubits 1 and 2) in the presence of the third qubit can be expressed as

$$C = \frac{2|g_1\Delta_2\Delta_3||g_2\Delta_1\Delta_3|}{(g_1\Delta_2\Delta_3)^2 + (g_2\Delta_1\Delta_3)^2 + (g_3\Delta_1\Delta_2)^2}, \quad (15)$$

where Δ_j and δ_j have the same form as the previous definition.

To avoid misleading readers, here, we have set the energy of the third qubit to be larger than that of the incident microwave-photon with the detuning $\delta_3 = -0.025g_2$, while $\delta_1 = -0.05g_2$ and $\delta_2 = +0.05g_2$. As can be seen in Fig. 5, in both the linear and the parabolic regimes of the dispersion relation, the Fano line shapes change when decreasing the coupling between the third qubit and the photon. This is because the larger difference between the couplings induces more diversity between the two channels, leading to the distinct Fano line shapes. The presence of the third qubit also induces additional interference of the discrete and continuous states. As a result, the transmission spectra show the double Fano line shapes in Fig. 5.

Figure 6 shows how the concurrence of the first two qubits changes when decreasing the coupling g_3. As seen, the quantum coherence moves back to the first two qubits (qubits 1 and 2) while reducing the coupling g_3. However, the presence of the third qubit does not affect the zero points of the concurrence. Since the general forms of the transmission coefficient and concurrence [Eqs. (14) and (15)] of the three-qubit case have a predictable rule, it is possible to extend the present theory to the case of the qubit array.

VI. SCATTERING PROPERTY OF A QUBIT ARRAY

The scattering property of a charge-qubit array coupled to the transmission resonators can be studied by applying the transfer-matrix method. For the case of a single-qubit coupled to the transmission resonators, the transmission amplitude t and the reflection amplitude r can be obtained by solving the eigenvalue equation [40]:

$$t = \cos\varphi e^{i\varphi}, \quad r = i\sin\varphi e^{i\varphi}, \quad (16)$$

where the phase shift $\varphi = \tan^{-1}(\frac{g^2}{\Delta})$, with g being the coupling strength between the field and the qubit, and Δ has been defined in Sec. III for both linear and parabolic dispersion relations. The transfer matrix T_q for the transmission resonators coupled to a single-qubit can be calculated from the Green's-function method [44] as

$$T_q = \frac{1}{t}\begin{bmatrix} t^2 - r^2 & r \\ -r & 1 \end{bmatrix} = \begin{bmatrix} 1 + i\epsilon & i\epsilon \\ -i\epsilon & 1 - i\epsilon \end{bmatrix}, \quad (17)$$

with $\epsilon = \tan\varphi$. We can extend this scheme to the qubit array case; the transfer matrix τ through the whole system can then be written as [45]

$$\tau = \prod_{i=1}^{N} T_{q_i} T_{d_i}, \quad (18)$$

where

$$T_d = \begin{pmatrix} e^{ikd_i} & 0 \\ 0 & e^{-ikd_i} \end{pmatrix} \quad (19)$$

represents the transfer matrix for the transmission resonator with length d_i. Note that the parameter ϵ in the transfer
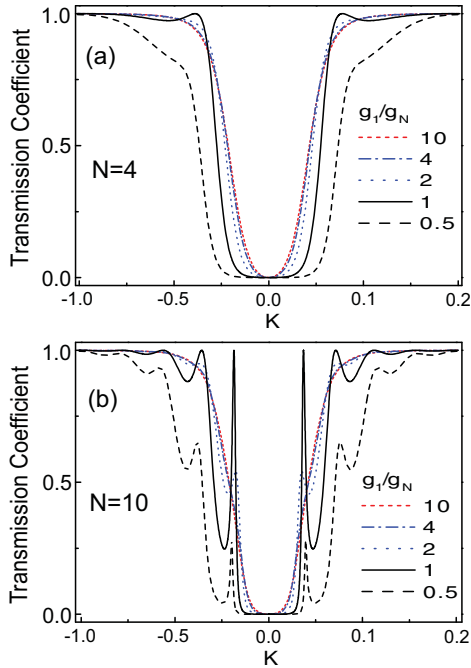
FIG. 7. (Color online) The transmission coefficient of the system consisting of the transmission resonators coupled to a N-charge-qubit array for (a) $N = 4$ and (b) $N = 10$. Here, the ratio of the coupling strength g_1 and other qubits g_i ($i \neq N$) is fixed to be 10, and g_1/g_N is varied. Parameters are normalized by g_2, and the normalized wave vector is defined as $K \equiv v_g k / g_2$.

VII. EXPERIMENTAL REMARKS

The correlation between the Fano resonance and bipartite entanglement has been reported [46] recently in a plasmonic system of a metal nanowire coupled to two quantum dots. In general, the nonlinear dispersion relation of the surface plasmons stems from the geometry of the nanowire, which generally cannot be changed without an external field [47]. In addition, to see the variations of the Fano resonance and concurrence, one needs to tune the energy and the couplings of the quantum dots. Therefore, it might not be easy to control the parameters experimentally. On the contrary, in the superconducting charge qubits coupled to the transmission-line resonators, the dispersion relation can be varied through the change of the interresonator coupling J, the coupling between the qubit and the microwave photon can be changed in the range of 5–200 MHz by varying the magnetic flux and the gate voltage [3], and the detuning between the transition frequency of the qubit and the microwave photon can be tuned in the same way from -10 to 10 GHz [3]. In this work, the coupling g_2 has been used as the unit to normalize all other parameters. We assume g_2 to be a feasible value around 20 MHz. Correspondingly, $g_1 = 200$ MHz, $\delta_2 = 1$ MHz, the hopping probability $J = 10$ MHz, and the minimum of the parabolic dispersion relation $\omega_c = 5$ GHz. By indicating the correlation between the Fano resonance and the two-qubit entanglement, we provide an easy way to estimate the entanglement through the measurement of the scattering spectra.

VIII. SUMMARY

In conclusion, we investigated the system consisting of two SQUID-based charge qubits placed near the coupled transmission-line resonators. We studied the scattering spectra of the microwave photon propagating in the coupled transmission line. The transmission coefficients in both linear and parabolic regimes of the dispersion relation show the Fano line shape. We further studied the entanglement between the two qubits and found that, when the Fano resonance occurs, the entanglement in both linear and parabolic regimes varies from unity to zero. This result indicates that a correlation exists between the Fano resonance and two-qubit entanglement. We also obtained the general forms of the transmission coefficient and the bipartite concurrence in the presence of the third charge qubit. By varying the coupling between the third qubit and the microwave photon, both the transmission and the entanglement can be controlled. The scattering property has also been extended to the system of the charge-qubit array; we found the propagation-forbidden region can be formed and controlled by varying the coupling strength or the number of qubits.

matrix T_{q_i} has been changed correspondingly to $\epsilon = \frac{g_i^2}{\Delta}$, with g_i being the coupling strength between the field and the ith qubit, and $d_N = 0$ for the transfer matrix T_{d_N} since the microwave photon is scattered at the Nth qubit. From the transfer matrix τ, the scattering coefficient for arbitrary coupling strength g_i and interqubit distance d_i can be obtained.

In the transmission spectrum, we find that with fixed interqubit distance $d_i = \pi/2$ and the energy detuning $\delta_i = 0.025g_2$, a propagation-forbidden region ($T = 0$) exists in the parabolic regime. In Fig. 7(a), we plot the transmission coefficient for qubit number $N = 4$ with a fixed ratio of the coupling strength $g_1/g_2 = g_1/g_3 = 10$ but with varying g_4. As can be seen, the propagation-forbidden region in the transmission spectrum becomes wider when increasing g_4. As a comparison, Fig. 7(b) shows the transmission spectra for qubit number $N = 10$. In plotting this panel, we fix the ratio of $g1$ to other coupling strengths g_j ($j = 2$–9) and vary the coupling g_{10}. Similarly, the propagation-forbidden region becomes wider with increasing g_{10}. However, compared with Fig. 7(a) ($N = 4$), the presence of the additional qubits significantly squeezes the propagation-forbidden region. This indicates that in a system of the transmission resonators coupled to a charge-qubit array, one can control the microwave photon to propagate or not either by tuning the coupling strength or switching on or off the coupling of some qubits.

[1] J. Q. You and F. Nori, Phys. Today **58**(11), 42 (2005).
[2] J. Q. You and F. Nori, Nature (London) **474**, 589 (2011).
[3] A. Wallraff, D. I. Schuster, A. Blais, L. Frunzio, R.-S. Huang, J. Majer, S. Kumar, S. M. Girvin, and R. J. Schoelkopf, Nature (London) **431**, 162 (2004).
[4] M. A. Sillanpää, J. I. Park, and R. W. Simmonds, Nature (London) **449**, 438 (2007).
[5] A. A. Houck *et al.*, Nature (London) **449**, 328 (2007).
[6] M. Hofheinz *et al.*, Nature (London) **459**, 546 (2009).
[7] D. P. DiVincenzo and J. A. Smolin, New. J. Phys **14**, 013051 (2012).
[8] J. Q. You and F. Nori, Phys. Rev. B **68**, 064509 (2003).
[9] I. Chiorescu *et al.*, Nature (London) **431**, 159 (2004).
[10] L. C. Hoi *et al.*, New. J. Phys **15**, 025011 (2013).
[11] J. Majer *et al.*, Nature (London) **449**, 443 (2007).
[12] Y. A. Pashkin *et al.*, Nature (London) **421**, 823 (2002).
[13] G. Romero, J. J. García-Ripoll, and E. Solano, Phys. Rev. Lett. **102**, 173602 (2009).
[14] B. Peropadre, G. Romero, G. Johansson, C. M. Wilson, E. Solano, and J. J. García-Ripoll, Phys. Rev. A **84**, 063834 (2011).
[15] Y.-F. Chen, D. Hover, S. Sendelbach, L. Maurer, S. T. Merkel, E. J. Pritchett, F. K. Wilhelm, and R. McDermott, Phys. Rev. Lett. **107**, 217401 (2011).
[16] S. Filipp *et al.*, Phys. Rev. Lett. **102**, 200402 (2009).
[17] M. D. Reed *et al.*, Nature (London) **482**, 382 (2012).
[18] D. Bozyigit *et al.*, Nat. Phys. **7**, 154 (2010).
[19] Y. Yin *et al.*, Phys. Rev. Lett. **110**, 107001 (2013).
[20] L. DiCarlo *et al.*, Nature (London) **460**, 240 (2009).
[21] C. Lang *et al.*, Phys. Rev. Lett. **106**, 243601 (2011).
[22] F. Mallet, F. R. Ong, A. Palacios-Laloy, F. Nguyen, P. Bertet, D. Vion, and D. Esteve, Nat. Phys. **5**, 791 (2009).
[23] W. C. Chien, C. S. Wu, and W. Kuo (private communication).
[24] U. Fano, Phys. Rev. **124**, 1866 (1961).
[25] A. E. Miroshnichenko, S. Flash, and Y. S. Kivshar, Rev. Mod. Phys. **82**, 2257 (2010).
[26] S. W. Kim and S. Kim, Phys. Rev. B **63**, 212301 (2001).
[27] S. Flach, A. E. Miroshnichenko, V. Fleurov, and M. V. Fistul, Phys. Rev. Lett. **90**, 084101 (2003).
[28] A. E. Miroshnichenko, Phys. Rev. E **79**, 026611 (2009).
[29] B. luk'yanchuk *et al.*, Nat. Mater. **9**, 707 (2010).
[30] A. E. Miroshnichenko and Y. S. Kivshar, Phys. Rev. E **72**, 056611 (2005).
[31] S. Flach, V. Fleurov, A. V. Gorbach, and A. E. Miroshnichenko, Phys. Rev. Lett. **95**, 023901 (2005).
[32] M. F. Yanik, S. Fan, M. Soljacic, and J. D. Joannopoulos, Opt. Lett. **28**, 2506 (2003).
[33] S. F. Mingaleev, A. E. Miroshnichenko, and Y. S. Kivshar, Opt. Express. **15**, 12380 (2007).
[34] S. F. Mingaleev, A. E. Miroshnichenko, and Y. S. Kivshar, Opt. Express. **16**, 11647 (2008).
[35] Q. Xu, S. Sandhu, M. L. Povinelli, J. Shakya, S. Fan, and M. Lipson, Phys. Rev. Lett. **96**, 123901 (2006).
[36] M. Kroner *et al.*, Nature (London) **451**, 311 (2008).
[37] L. Zhou, Z. R. Gong, Y. X. Liu, C. P. Sun, and F. Nori, Phys. Rev. Lett. **101**, 100501 (2008).
[38] L. Zhou, H. Dong, Y. X. Liu, C. P. Sun, and F. Nori, Phys. Rev. A **78**, 063827 (2008).
[39] D. E. Chang, A. S. Sørensen, E. A. Demler, and M. D. Lukin, Nat. Phys. **3**, 807 (2007).
[40] J. T. Shen and S. Fan, Phys. Rev. Lett. **95**, 213001 (2005).
[41] W. Chen, G. Y. Chen, and Y. N. Chen, Opt. Exp. **18**, 10360 (2010).
[42] S. John and T. Quang, Phys. Rev. A **50**, 1764 (1994).
[43] W. K. Wootters, Phys. Rev. Lett. **80**, 2245 (1998).
[44] S. Fan, P. R. Villeneuve, J. D. Joannopoulos, M. J. Khan, C. Manolatou, and H. A. Haus, Phys. Rev. B **59**, 15882 (1999).
[45] M. F. Yanik, W. Suh, Z. Wang, and S. Fan, Phys. Rev. Lett. **93**, 233903 (2004).
[46] G. Y. Chen and Y. N. Chen, Opt. Lett. **37**, 4023 (2012).
[47] W. Chen, G. Y. Chen, and Y. N. Chen, Opt. Lett. **36**, 3602 (2011).